American Journal of Nanosciences
2018; 4(4): 40-45
http://www.sciencepublishinggroup.com/j/ajn
doi: 10.11648/j.ajn.20180404.11
ISSN: 2575-484X (Print); ISSN: 2575-4858 (Online)

Preparation, Characterization and Photocatalytic Application of Sol-Gel Synthesis of Co Doped TiO_2

Nadarajan Suresh Babu[1], Arumugam Vijayabalan[2, *], Ramasamy Shankar[2]

[1]Department of Chemistry, Government College of Engineering, Thanjavur, India

[2]Department of Chemistry, St. Joseph's College of Arts and Science (Autonomous), Cuddalore, India

Email address:
vijayabalanchem@gmail.com (A. Vijayabalan)

[*]Corresponding author

To cite this article:
Nadarajan Suresh Babu, Arumugam Vijayabalan, Ramasamy Shankar. Preparation, Characterization and Photocatalytic Application of Sol-Gel Synthesis of Co Doped TiO_2. *American Journal of Nanosciences*. Vol. 4, No. 4, 2018, pp. 40-45. doi: 10.11648/j.ajn.20180404.11

Received: December 31, 2018; **Accepted**: January 14, 2019; **Published**: February 26, 2019

Abstract: Nano Co doped TiO_2 prepared by simple impregnation method and characterized by powder XRD, high resolution scanning electron micrograph, diffuse reflectance spectroscopy, photoluminescence spectroscopy and infra-red spectroscopy. DRS reveal that the absorption of TiO_2 wavelength is shifted to visible region when Co^{2+} ion doped. PL spectra show that the emission of light is higher and the liberation of iodine is more for Co doped TiO_2 than TiO_2. Application of this catalyst is degradation of MB dye under visible light.

Keywords: Impregnation Method, Co Doped TiO_2, Visible Light, MB Dyes

1. Introduction

Photocatalytic semiconductor is one of the promising techniques for the disinfection of bacteria and degradation of organic dyes [1–9]. TiO_2 is an efficient for photocatalytic application because of its exceptional electronic and optical properties, chemical stability, non-toxicity, and low cost. However, it requires UV-A light for photo activation and the overall quantum efficiency is low. In order to improve the photo efficiency of the TiO_2 doped with transition metal is being widely employed. The origin of the improved photocatalytic activity is clearly related to the efficiencies of the doping centers in trapping charge carriers and interceding in the interfacial transfer. Besides modifying the band gap, metal ions also serve as charge trapping sites and thus reduce electron–hole recombination rates. The effect of doping on the activity depends on many factors, like the type and the concentration of dopant, the method of doping, etc. One of the most promising ideas to extend the light absorbing property of TiO_2 and to enhance its photocatalytic efficiency is to couple TiO_2 with a narrow band gap semiconductor. In these circumstances, both semiconductors must have their conduction as well as valence band edges at different energy levels. Under such configuration, several advantages can be obtained. Some is: (1) an improvement of charge separation; (2) an increase in the life time of the charge carrier; and (3) an enhancement of the interfacial charge transfer efficiency to adsorbed substrate. Some properties of TiO_2 nanostructures, like photocatalytic activity, strongly depend on the degree of crystallinity and crystalline structure, morphology, particle size, size distribution, specific surface area, surface states, and porosity [10-12]. Anatase, is regarded as the most active polymorph of TiO_2, shows higher affinity to adsorb organic molecules compared to rutile [13, 14]. Transition metal doping is favorable because of transition metal's unique'd' electronic configuration and spectral characteristics of extending the absorption edge of TiO_2 to the visible region [15, 16]. Doping with metal or non-metal elements could shift the light absorption edge from UV to the visible region. Thus, the photo response is enhanced by creating mid-gap energy levels in the band gap of TiO_2 [17, 18]. Nonmetals such as N [19], S [14], and B [20] and metals like Cu [21], Pt [22], Ag [23], and Fe [19, 10, 24], etc. have been studied for the promotion of photocatalytic activity of TiO_2 in both UV and visible light irradiation. Photocatalytic activity and magnetic properties of Co doped TiO_2at room temperature is better than neat TiO_2 [25-27]. Removal of cyanide ion by Co doped TiO_2 was studied [28]. Doped TiO_2 with Co is considered as one of the

best candidates to reduce the electron–hole recombination rate and to shift the absorption edge into the visible light region [29-31]. Cobalt doped TiO2 has shown high activity for degradation of 2-chlorophenol (2-CP) [32], 4-CP and Bisphenol A [33], acetaldehyde [34-36], acetonitrile [37], methylorange [25], methylene blue [38, 39], rhodamine B [40] and azofuchsine [41].

In the present study are investigating the degradation of methylene blue dye by Co doped TiO_2 under visible light and characterization of this catalyst.

2. Materials and Methods

2.1. Materials

Co $(NO_3)_2$ (Hi-media) and TiO_2 (Merck) Methylene blue dye (Merck) and Ethanol solution were used.

2.2. Preparation of Co Doped TiO_2 By Impregnation Method

To 15 ml of 99.9% purity of ethanol were taken in the beaker and appropriate amount of TiO_2 was added into the ethanol solution under stirring for 30 min. 0.05g of Cobalt nitrate were added to the TiO_2 containing solution also with stirring. This mixture is evaporated at 60°C for 30 min with stirring.

2.3. Analysis

A PANalyticalX'Pert PRO diffractometer with Cu Ka rays of 1.5406 Å was employed to record the powder X-ray diffractograms (XRD) of the samples at 40 kV and 30 mA with a scan rate of $0.04°s^{-1}$ in a 2Θ range of 10–75°. The morphologies of Co doped $TiO_2$was assessed using a FEI Quanta 200 high resolution scanning electron microscope (HR-SEM) under highvacuum mode. The diffuse reflectance spectra were obtained with a PerkinElmer Lamda 35 spectrometer. A PerkinElmer LS 55 fluorescence spectrometer was used to record the photoluminescence (PL) spectra at room temperature. The stretching and bending vibration of atom are studied by FT-IR spectrophotometer. The doped catalyst were dispersed in carbon tetrachloride and excited at 300 nm. The decolourisation and degradation of dyes are evaluated by UV-visible spectrophotometer.

2.4. Photocatalytic Activity

The visible light photocatalytic studies were made in an immersion type photo reactor equipped with a 150-W tungsten halogen lamp fitted into a double walled borosilicate immersion well of 40 mm outer diameter with inlet and outlet for circulation of $K_2Cr_2O_7$ solution. The 1N $K_2Cr_2O_7$ solution used removes 99 % of the UV light with wavelength between 320 and 400 nm and acts as a UV cutoff filter. After the addition of the catalyst to the dye solution, air was bubbled through the solution which kept the catalyst particles under suspension and at constant motion. The catalyst was separated after the illumination. The Methylene blue dye was analyzed spectrophotometrically at 625 nm.

3. Results and Discussion

3.1. Crystal Structure

The X-ray diffraction pattern of Co-doped TiO_2 are prepared by simple impregnation method is shown in figure 1. It reveals the crystal structure of the Co doped TiO_2 as tetragonal body centered with crystal constants *a* and*b* as 0.3777 nm and *c* as 0.9501 nm. The diffraction pattern matches totally with the standard JCPDS pattern of rutile (89-8304). The absence of anatase lines (21-1272)in the cobalt doped TiO_2; the reason is at high temperature anatase TiO_2 is converted to rutile TiO_2. Further, the diffraction peaks of CoO absence at doped TiO_2. The low composition of Co may also be a reason for the absence of CoO peak in the XRD of Co-doped TiO_2. Hence it is inferred that the doping has not resulted in substitution of the smaller Ti^{4+} by the larger Co^{2+} in the crystal lattice. Figure 1 also displays the XRD of the undoped TiO_2. The diffraction pattern of the undoped TiO_2 shows the presence of anatase phases only (JCPDS 21-1272). The phase percentages of anatase and rutile have been deduced from the integrated intensity of the peaks at 2θ value of 25.3° for anatase and 27.4º for rutile. The percentage of anatase is given by $A\ (\%) = 100/\ \{1 + 1.265(I_R/I_A)\}$, where I_A is the intensity of the anatase 101-peak at $2\theta = 25.3º$ and I_R is that of the rutile 110-peak at $2\theta = 27.4º$. The phase composition thus obtained is 83% anatase. The average crystallite sizes (D) of the Co-doped TiO_2 and undoped TiO_2 have been obtained from the half-width of the full maximum (HWFM) of the most intense peaks of the respective crystals using the Scherrer equation $D = 0.9\lambda/\beta\cos\theta$, where D is the average crystallite size, λ is the wavelength of X-rays used, θ is the diffraction angle and β is the full width at half maximum of the peak. The crystallite size of the Co-doped TiO_2 is larger than the undoped one and the results are presented in Table 1. The specific surface areas of the crystals have been obtained using the relationship, $S = 6/\rho D$, where S is the specific surface area, D is the average particle size and ρ is the material density. The results are in accordance with the crystal size and are presented in Table 1.

Table 1. *Crystal size (D) and Surface area (S) of $TiO_2$and Co-TiO_2.*

Oxide	***D*, nm**	***S*, m^2g^{-1}**
TiO_2	9.9	143
Co-$TiO_2$14.9		95

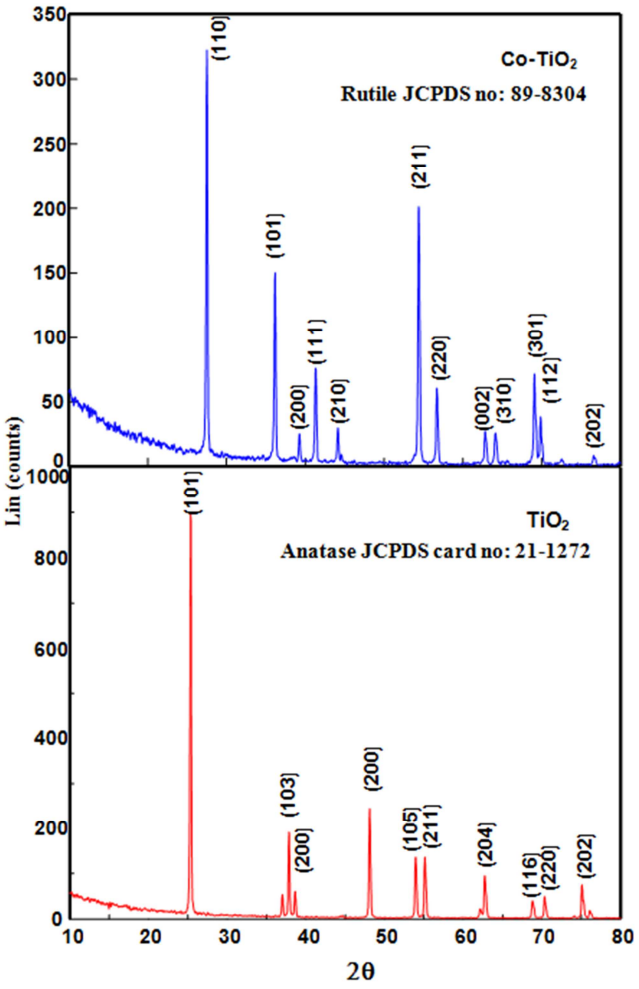

Figure 1. *Powder XRD spectra of TiO_2 and Co doped TiO_2..*

3.2. Morphology

Figure 2 High resolution scanning electron microscope (HR-SEM) shows that the TiO_2 particles are spherical and 9.9nm. But Co^{2+} ion impregnate to TiO_2 lattice agglomerate the particles and become the 14.9.

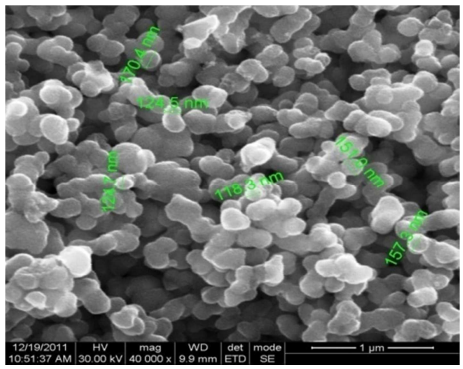

Figure 2. *HR-SEM image of Co doped TiO_2.*

3.3. Diffuse Reflectance Spectroscopy

The diffuse reflectance spectra of pure TiO_2 and Co doped TiO_2 are shown in figure 3. In Co doped TiO_2 has higher absorption in visible region compare to bare TiO_2. Figure 4 are shows that the Tauc plot for direct bandgap energy of TiO_2 and Co doped TiO_2 are 3.4 and 2.95 eV respectively. The direct band gap energy of TiO_2 is 3.4eV, the wavelengths of TiO_2 are shifted from UV region to visible region when Co^{2+} ion intercalated TiO_2 lattice.

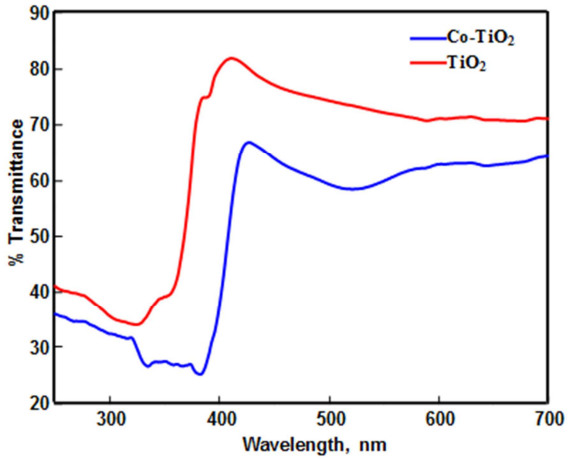

Figure 3. *DRS spectra of$TiO_2$and Co doped TiO_2.*

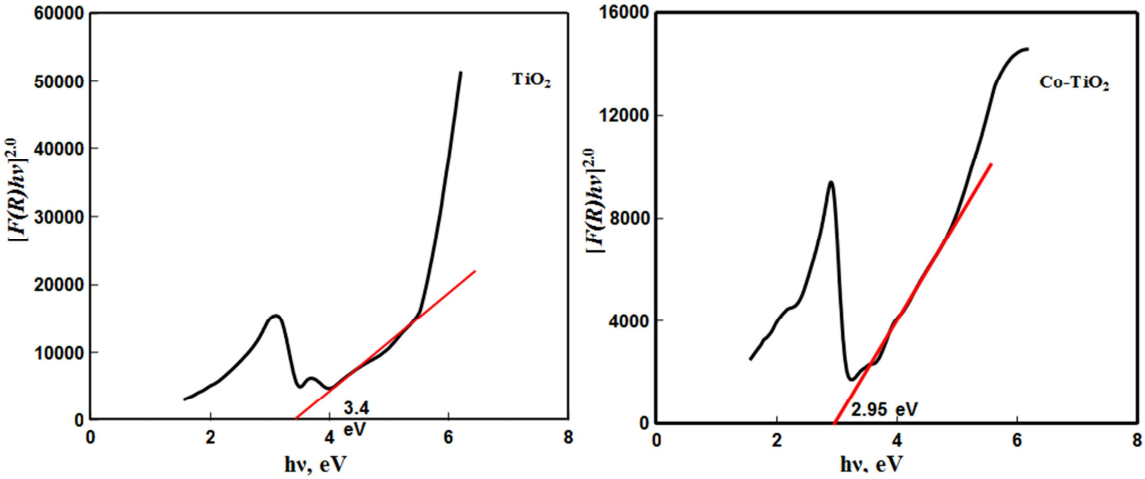

Figure 4. *Tauc plot for direct bandgap energy of TiO_2 and Co doped TiO_2.*

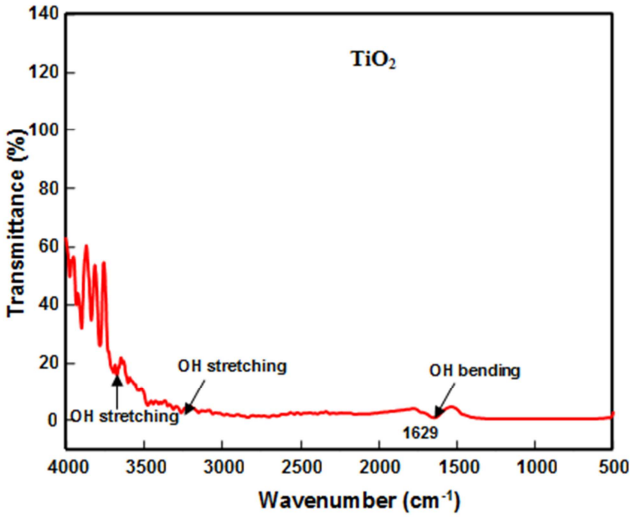

Figure 5. *PL spectra of TiO_2 and Co doped TiO_2.*

3.4. Emission Spectroscopy

The photoluminescence (PL) spectra of the bare TiO_2 and Co doped TiO_2 are shown in figure 5. Photoluminescence occurs due to the recombination of electron–hole pair in the semiconductor. The excitation wavelength is 300nm. The recombination of electron-hole pair in Co doped TiO_2 are faster than pure TiO_2.

3.5. FT-IR Spectroscopy

FT-IR spectroscopy is a useful tool to help understand the behavior of functional group. The infrared spectra of TiO_2 and Co doped TiO_2 are shown in figure 6. The peaks around 3350–3450 and 1620–1635 cm^{-1} in Figure 6 were assigned to stretching vibrations and bending vibrations of the O–H, respectively, which may come from the surface absorbed water. The vibrations of O–H were significantly weaker, which was related to the removal of water after calcinations during the preparation of Co doped TiO_2. The weak peak at about 514cm^{-1} assigned to stretching vibrations of Co–O. FT-IR results reminded the formation of a small part of Co–O bond. It was probably the existence of Co–O bond that hindered the recombination of generated photo holes and photoelectrons [42].

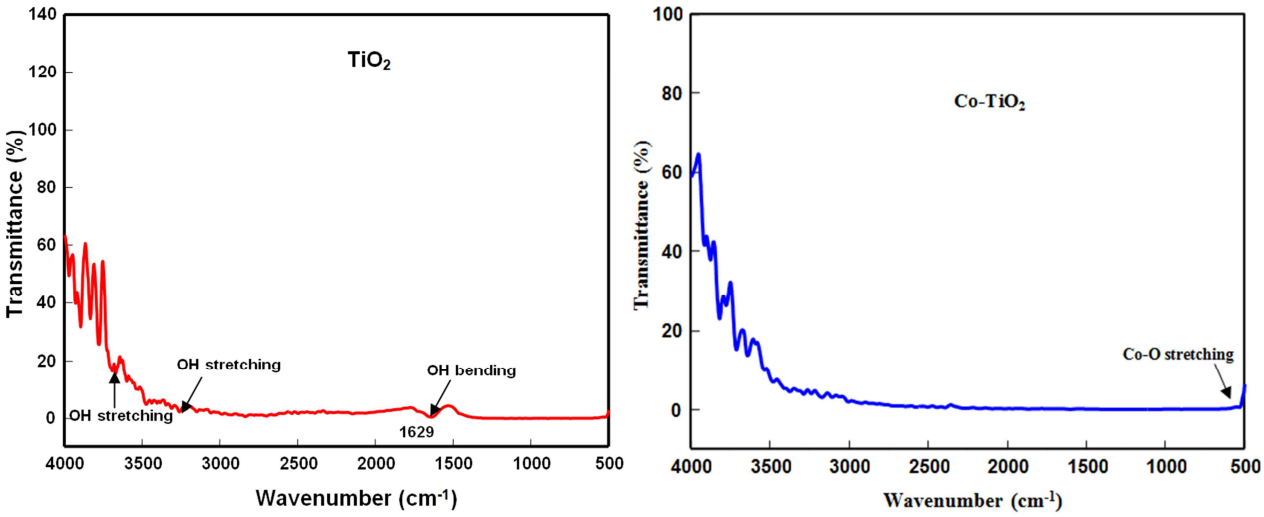

Figure 6. *FT-IR spectra of TiO_2 and Co doped TiO_2.*

3.6. Dye Degradation

The temporal profiles degradation of methylene blue dye by TiO_2 and Co doped TiO_2 under visible light is shown in figure 7. The Co doped TiO_2 is more efficient photocatalytic degradation of methylene blue dye than TiO_2. This might be due to trapping photo-excited electrons at conduction band by decreasing the electron-hole recombination as a consequence of Co dopant into TiO_2 environment. Doping has regulated the degradation occurred by exhibiting the highest photo catalytic degradation efficiency in methylene blue dye. This is because the incorporated Co atom acts as electron traps by suppressing the recombination of photo-generated holes and electrons. Both superoxide radicals and hydroxyl radicals are responsible degradation of methylene blue dye. Figure 8 are shows that photocatalytic mechanism for organic dye.

3.7. Oxidation of Iodide Ion

Figure 9 Shows that liberation of iodine from oxidation of iodide ion solution by Co doped TiO_2 more enhancement than pure TiO_2 under visible light at 60 minutes.

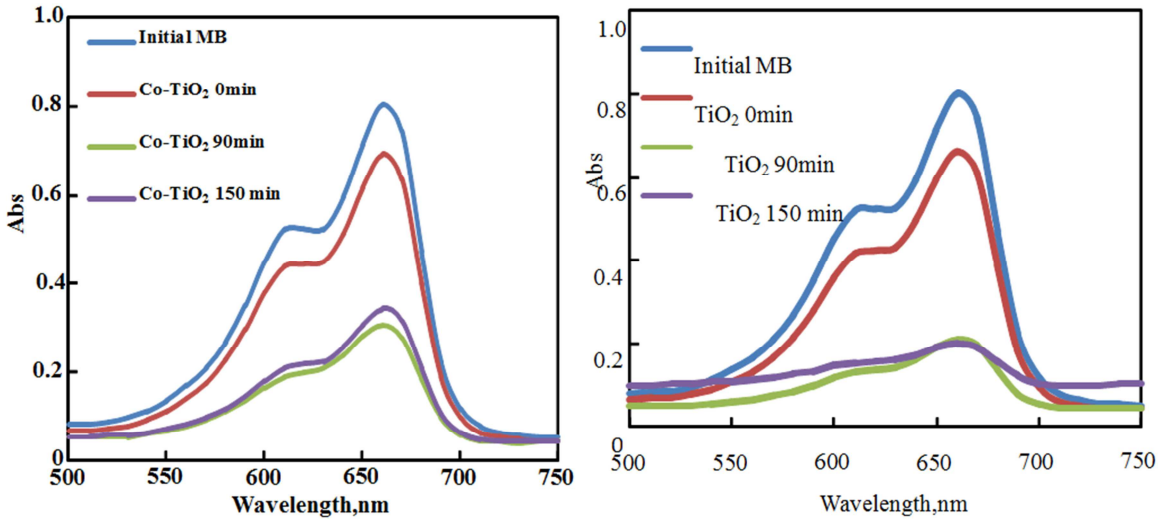

Figure 7. *Time profile degradation of MB dye under visible light.*

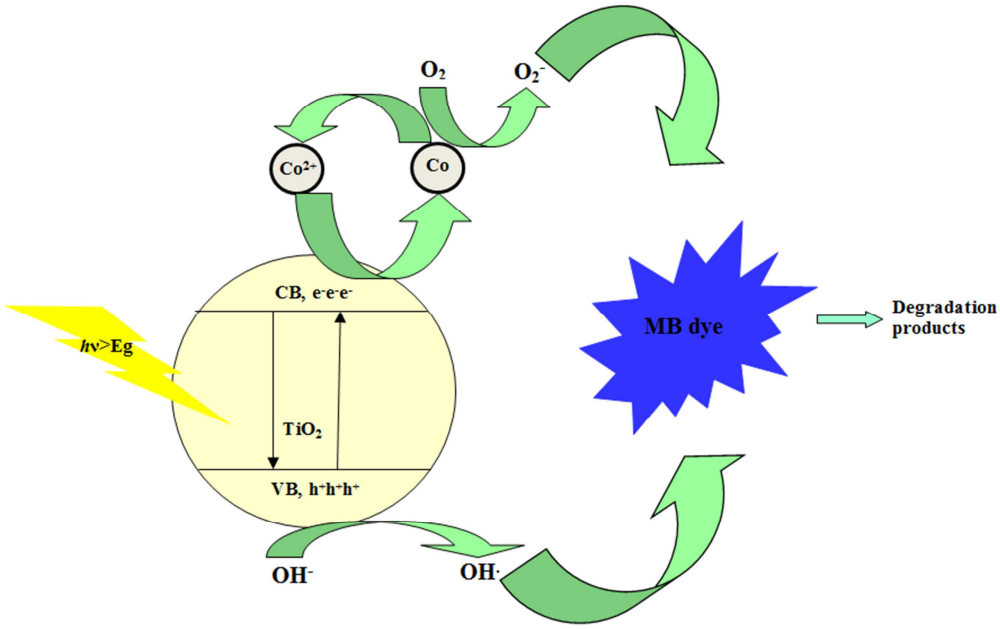

Figure 8. *Mechanism of degradation of organic dye by Co doped TiO_2 under visible light.*

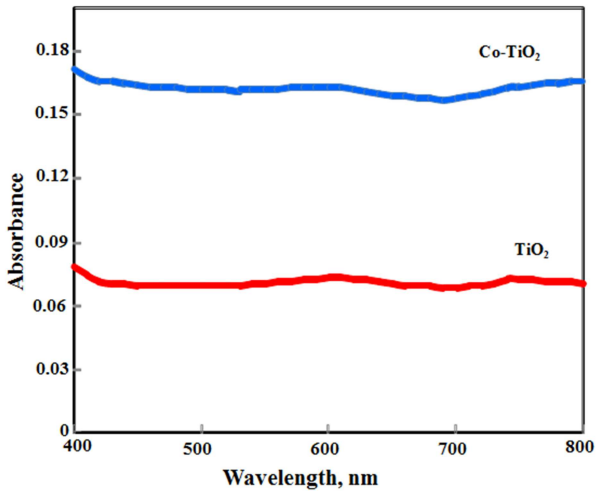

Figure 9. *Photocatalytic oxidation of iodide ion by TiO_2 and Co doped TiO_2.*

4. Conclusions

The Co doped TiO_2 prepared by impregnation method. DRS show that the optical edge of TiO_2 is shifted to visible region when Co^{2+} ion doped. PL reveals that the Co doped TiO_2 lattice more emission of light due to crystal defect and less emission of light for TiO_2 due to enhance the crystallinity. Application of this catalyst is degradation of MB dyes under visible light.

References

[1] J. A. Rengifo-Herrera, C. Pulgarin, Sol. Energy, 84, 37 (2010).

[2] J. A. Rengifo-Herrera, K. Pierzchala, A. Sienkiewicz, L. Forro, J. Kiwi, J. E. Moser, C. Pulgarin, J. Phys. Chem. C, 114, 2717 (2010).

[3] J. A. Rengifo-Herrera, E. Mielczarski, J. Mielczarski, N. C. Castillo, J. Kiwi, C. Pulgarin, Appl. Catal. B, 84, 448, (2008).

[4] J. A. Rengifo-Herrera, K. Pierzchala, A. Sienkiewicz, L. Forro, J. Kiwi, C. Pulgarin, Appl. Catal. B,88, 398, (2009).

[5] Y. Liu, J. Li, X. Qiu, C. Burda, J. Photochem. Photobiol., A 190, 94, (2007).

[6] C. Karunakaran, G. Abiramasundari, P. Gomathisankar, G. Manikandan, V. Anandi, Mater. Res. Bull. 46, 1586, (2011).

[7] C. Karunakaran, G. Abiramasundari, P. Gomathisankar, G. Manikandan, V. Anandi, J. Am. Ceram. Soc. 94, 2499, (2011).

[8] C. Karunakaran, G. Abiramasundari, P. Gomathisankar, G. Manikandan, V. Anandi, J. Colloid, Interface Sci. 352, 68, (2010).

[9] C. Karunakaran, A. Vijayabalan, G. Manikandan, P. Gomathisankar, Catal. Commun. 12, 826, (2011).

[10] H.-J. Lin, T.-S. Yang, C.-S. Hsi, M.-C. Wang, K.-C. Lee, Ceram. Intern. l, 40, 10633-10640, (2014).

[11] M. Rashad, E. Elsayed, M. Al-Kotb, A. Shalan, J Alloys and Compounds, 581, 71-78, (2013).

[12] J.-Y. Park, K.-I. Choi, J.-H. Lee, C.-H. Hwang, D.-Y. Choi, J.-W. Lee, Mater. Lett., 97, 64-66(2013).

[13] M. Nasir, S. Bagwasi, Y. Jiao, F. Chen, B. Tian, J. Zhang, Chem. Eng., J, 236, 388-397(2014).

[14] C. McManamon, J. O'Connell, P. Delaney, S. Rasappa, J. D. Holmes, M. A. Morris, J Mol. Catal. A: Chemical, 406, 51-57, (2015).

[15] A. Siddiqa, D. Masih, D. Anjum, M. Siddiq, J Environ. Sci., 37, 100-109, (2015).

[16] Y. Wang, R. Zhang, J. Li, L. Li, S. Lin, Nano. Res. Let., 9,1-8, (2014).

[17] J. Wang, Y. Zhao, T. Wang, H. Li, C. Li, PhysicaB: Cond., Matter, 478, 6-11, (2015).

[18] L. Samet, J. B. Nasseur, R. Chtourou, K. March, O. Stephan, Mat. Character. 85, 1-12, (2013).

[19] S. Larumbe, M. Monge, C. Gómez-Polo, Appl. Surf. Sci., 327, 490-497, (2015).

[20] S. In, A. Orlov, R. Berg, F. García, S. Pedrosa-Jimenez, M. S. Tikhov, D. S. Wright, R. M. Lambert, J Amer. Cemical. Society, 129, 13790-13791, (2007).

[21] F. Gonell, A. V. Puga, B. Julián-López, H. García, A. Corma, Appl. Catal. B: Environ. 180, 263-270, (2016).

[22] Y. Hu, X. Song, S. Jiang, C. Wei, Chem. Eng. J., 274, 102-112, (2015).

[23] S. Kment, H. Kmentova, P. Kluson, J. Krysa, Z. Hubicka, V. Cirkva, I. Gregora, O. Solcova, L. Jastrabik, J. Coll. Int. Sci., 348, 198-205, (2010).

[24] W. Tang, X. Chen, J. Xia, J. Gong, X. Zeng, Mat. Sci., Eng. B, 187, 39-45(2014).

[25] M. Hamadanian, A. Reisi-Vanani, A. Majedi, J. Iran. Chem. Soc. 7, S52, (2010).

[26] C. Shifu, L. Wei, Z. Sujuan, C. Yinghao, J. Sol–Gel Sci. Technol., 54, 258, (2010).

[27] M. Subramanian, S. Vijayalakshmi, S. Venkataraj, R. Jayavel, Thin Solid Films516, 3776, (2008).

[28] Elham S. Baeissa, J. Ind. Eng., Chem., (2014)

[29] P. N. Kapoor, S. Uma, S. Rodriguez, K. J. Klabunde, J. Mol. Catal. A Chem. 229, 145‑150, (2005).

[30] M. A. Barakat, H. Schaeffer, G. Hayes, S. Ismat-Shah, Appl. Catal. B 57, 23‑30 (2005).

[31] Q. J. Yang, H. Choi, Y. J. Chen, D. D. Dionysiou, Appl. Catal. B 77, 300‑307 (2008).

[32] M. A. Barakat, H. Schaeffer, G. Hayes, S. Ismat-Shah, Appl. Catal. B: Environ. 57, 23–30, (2005).

[33] R. Amadelli, L. Samiolo, A. Maldotti, A. Molinari, M. Valigi, D. Gazzoli, Int. J. Photo., 2008, 1–9, (2008).

[34] P. N. Kapoor, S. Uma, S. Rodriguez, K. J. Klabunde, J. Mol. Catal. A: Chem. 229, 145–150, (2005).

[35] D. B. Hamal, K. J. Klabunde, J. Phys. Chem. C 115, 17359–17367(2011).

[36] M. Iwasaki, M. Hara, H. Kawada, H. Tada, S. Ito, J. Colloid Interface Sci. 224, 202–204, (2000).

[37] S. N. R. Inturi, T. Boningari, M. Suidan, P. G. Smirniotis, Appl. Catal. B: Environ. 144, 333–342(2014).

[38] B. Qi, Y. Yu, X. He, L. Wu, X. Duan, J. Zhi, Mater. Chem. Phys. 135,549–553, (2012).

[39] I. Ganesh, A. K. Gupta, P. P. Kumar, P. S. C. Sekhar, K. Radha, G. Padmanabham, G. Sundararajan, Mater. Chem. Phys. 135, 225–234, (2012).

[40] Q. Chen, F. Ji, T. Liu, P. Yan, W. Guan, X. Xu, Chem. Eng. J. 229, 57–65, (2013).

[41] J. Wang, Y. Lv, Z. Zhang, Y. Deng, L. Zhang, B. Liu, R. Xu, X. Zhang, J. Hazard. Mater. 170, 398–404(2009).

[42] Jing Yang, Shihai Cui, Jun-qinQiao, Hong-zhen Lian, J Mol. Catal. A: Chemical, 395, 42–51(2014).